

This work was written as part of one of the author's official duties as an Employee of the United States Government and is therefore a work of the United States Government. In accordance with 17 U.S.C. 105, no copyright protection is available for such works under U.S. Law.

Public Domain Mark 1.0

<https://creativecommons.org/publicdomain/mark/1.0/>

Access to this work was provided by the University of Maryland, Baltimore County (UMBC) ScholarWorks@UMBC digital repository on the Maryland Shared Open Access (MD-SOAR) platform.

Please provide feedback

Please support the ScholarWorks@UMBC repository by emailing scholarworks-group@umbc.edu and telling us what having access to this work means to you and why it's important to you. Thank you.

Dynamics of southwest Asian dust particle size characteristics with implications for global dust research

Jeffrey S. Reid,¹ Elizabeth A. Reid,¹ Annette Walker,¹ Stuart Piketh,² Steve Cliff,³ Abdulla Al Mandoos,⁴ Si-Chee Tsay,⁵ and Thomas F. Eck⁵

Received 21 December 2007; revised 21 March 2008; accepted 13 May 2008; published 25 July 2008.

[1] As part of the United Arab Emirates Unified Aerosol Experiment (UAE²), the size distribution and chemistry of dust particles were measured for the months of August and September 2004 at an Arabian Gulf coastal site impacted by dust from several sources within southwest Asia. The characteristics of common mode dust ($0.8 < d_p < 10 \mu\text{m}$) were examined using an aerodynamic particle sizer (APS), a DRUM cascade impactor, and AERONET Sun/sky retrievals. While size properties from these distinct methods do correlate, accurate dust measurement is still an outstanding challenge. But when instruments are applied consistently in the correct context, the dynamics of dust particle size can be accurately studied. Here, observations are used to study the stability of dust size and chemistry characteristics. We found that dust particle size, chemistry, and morphology appear to be fairly static from individual sources, confirming preliminary hypotheses based on large-scale observations of Saharan dust. Thus, our data provide experimental evidence that on regional scales, common mode dust is not functionally impacted by production wind speed, but rather influenced by soil properties such as geomorphology or roughness length. Similarly, we found transport processes from the mesoscale to near synoptic scale do not significantly impact common mode dust size either. When combined with other APS observations around the world, the dust coarse mode is found to be fairly robust with a volume median diameter on the order of $\sim 3.5 \mu\text{m} \pm 30\%$. Finally, evidence for a strong submicron dust mode, suggested in previous studies, was inconclusive.

Citation: Reid, J. S., E. A. Reid, A. Walker, S. Piketh, S. Cliff, A. Al Mandoos, S.-C. Tsay, and T. F. Eck (2008), Dynamics of southwest Asian dust particle size characteristics with implications for global dust research, *J. Geophys. Res.*, 113, D14212, doi:10.1029/2007JD009752.

1. Introduction and Rationale

[2] In the fields of atmospheric science, ecology, and oceanography, the uncertainties in airborne dust monitoring and modeling are universally recognized. Coarse mode particles are difficult to measure, and for complicated dust particles there are massive divergences in sizing bias by method (aerodynamic, optical, geometric, retrieval) sometimes up to a factor of two [e.g., Reid *et al.*, 2003, 2006; Reid and Peters, 2007]. Sizing errors impact several modeled parameters, including optical properties, deposition rates, available surface area for chemical reactions, and even the most basic parameters such as dust mass concentration. A

fundamental consequence of sizing bias between methods is that it is difficult to compare measurements from studies over the globe and develop a consistent picture of the nature of airborne dust.

[3] Outstanding issues relevant to dust production, transport, and predictability include the following: (1) How much does dust size distribution differ between source regions? (2) For a given production zone, how much change is there in size or chemistry between or during events? (3) Can wind speed dependence be observed for the coarse mode properties? (4) Is there a robust submicron dust mode? (5) How much does dust size distribution change during transport?

[4] There are a number of hypothesized physical influences on dust size distribution and relative modal strengths. Certainly local geomorphology is a significant factor, as is the availability of saltators [Gillette and Chen, 1999; Gillette *et al.*, 2001; Alfaro and Gomes, 2001]. It has also been suggested that surface roughness length, wind speed, and friction velocity influence the coarse mode size [Alfaro and Gomes, 2001], although the extent to which these factors influence dust production regionally is unclear.

[5] Fortunately, a number of investigators have found that dust properties have commonalities, and there are some

¹Marine Meteorology Division, Naval Research Laboratory, Monterey, California, USA.

²Climatology Research Group, University of Witwatersrand, Johannesburg, South Africa.

³Department of Land, Air and Water Resources, University of California, Davis, California, USA.

⁴Department of Atmospheric Studies, Ministry of Presidential Affairs, Abu Dhabi, United Arab Emirates.

⁵NASA Goddard Space Flight Center, Greenbelt, Maryland, USA.

simplifications that we may be able to assume [Patterson and Gillette, 1977]. In particular, it appears that the size distribution of dust from any given source is remarkably stable. For example, Maring *et al.* [2003] found that the coarse mode (also referred to as “common mode”, here defined as $0.8 < d_p < 10$) size distribution of African dust measured in 2001 in Puerto Rico was extraordinarily similar to measurements made in Izania, Tenerife, several years earlier, with a geometric volume median diameter of $\sim 3.5\text{--}4.2\text{ }\mu\text{m}$. Similar hypotheses have been made regarding African dust mineralogy [Glaccum and Prospero, 1980; Prospero, 1981; Reid *et al.*, 2003]. There also appears to be a converging dust size distribution after several thousand kilometers of transport [Prospero *et al.*, 1989].

[6] One difficulty in applying these studies is that, with the exception of Maring *et al.* [2003], consistent measurements were not made across different dust sources and transport distances. To resolve outstanding issues, the United Arab Emirates Unified Aerosol Experiment (UAE²) provided a good context for the study of the size properties of atmospheric dust. As discussed by J. S. Reid *et al.* [2008] and A. Walker *et al.* (A study of metrological phenomenon during UAE², manuscript in preparation, 2008), the southern Arabian Gulf is a crossroads of a number of source regions and chemistries. Local dust can be measured one day, and as the large-scale flow patterns change, dust transported from over 1000 km away can be measured the next, thus providing a unique opportunity to consistently study the size distribution of dust from a number of distinct sources.

[7] Here we give an overview of the size properties of dust measured in the Arabian Gulf region during UAE² and examine the hypothesis that the dust coarse/common mode size distribution is fairly invariant from individual dust sources. The measurement methods include those that appeared to have some efficacy from previous studies [e.g., Reid *et al.*, 2003]: aerodynamic particle sizer, cascade impactor, and AERONET inversions. We recognize that the intercomparison of dust properties made by different instruments is extremely complicated (a topic of a forthcoming paper). But given the experiment design presented here, significant progress can be made in the field without a full reconciliation of instrument measurements.

2. Methods

[8] UAE² took place in the southern Arabian Gulf region in August and September 2004. The primary surface site utilized for the study reported here was the Mobile Atmosphere Aerosol and Radiation Characterization Laboratory (MAARCO), located 50 km north of Abu Dhabi, UAE (Lat. 24.7 N; Long. 54.65 E). The site was away from city plumes, and the air masses sampled there were representative of the Arabian Gulf and the interior desert. The MAARCO site contained a set of meteorology, radiation, remote sensing, particle size, chemistry, scattering, and absorption instruments. Here we use in situ sizing measurements as well as regional AERONET retrievals. Sampling of all instruments at MAARCO was performed through a common total suspended particulate matter (TSP) inlet running at ~ 220 lpm leading to a 0.3 m^3 mixing chamber. We expect the inlet and distribution system has a cut point

somewhere around $10\text{ }\mu\text{m}$. Relevant measurements are discussed below.

2.1. Filter Sampling

[9] In UAE² we utilized 24-h fine and TSP filter measurements that were made each day for the period 11 August to 30 September 2004. Complete descriptions of these procedures are given by E. A. Reid *et al.* (Chemical and morphological properties of southwest Asian dust, manuscript in preparation, 2008). Teflon filters were analyzed by gravimetry, X-ray fluorescence (XRF), and ion chromatography at the Desert Research Institute, Nevada. For source identification we use the Ca to Fe ratio as a rough indicator of carbonate to clay/silicate dust species, as well as other trace elements.

2.2. TSI Aerodynamic Particle Sizer 3321

[10] Continuous coarse mode size distributions were measured using a TSI aerodynamic particle sizer model 3321, which does not suffer from the anomalous $>10\text{ }\mu\text{m}$ peak seen in the earlier 3320 model [Stein *et al.*, 2002]. The APS fed from the common inlet through a heated ($\text{RH} < 35\%$) line. Several papers have discussed APS sampling efficiency issues [Volckens and Peters, 2005; Reid and Peters, 2007]. On the basis of these papers no nozzle or counting efficiency corrections appear necessary for dry dust.

[11] One aspect of the APS we must be mindful of is its response function to dense or asymmetric particles such as dust. Marshall *et al.* [1991] and Cheng *et al.* [1990, 1993] have suggested that the APS undersizes particles with irregular shapes, even those with dynamic shape factors as little as 1.1 (see Wang *et al.* [2002] for a synthesis). Conversely, the APS oversizes dense particles [Baron, 1996]. For particles such as dry dust, these effects offset and partly cancel each other, but ultimately may result in undersizing as large as 10–30% [Cheng *et al.*, 1993].

[12] The response of the APS to dust is complicated, and requires an entirely separate paper to convey our findings. Despite issues surrounding APS-like instruments, it is the authors' opinion that at the time of the UAE² study there was no other commercially viable option for studying rapid changes in dust particle size distributions at high size resolution. Indeed the APS is now probably the most commonly used instrument for measuring dust size. For consistency, our analysis is restricted to the instrument's indicated aerodynamic diameter (d_{aei}), to be distinguished from true aerodynamic diameter (d_{ae}). By taking the APS on its own terms, we can sequester the issues related to the measurement of “true size” in favor of investigating dust size variability. Indeed, the strong nonlinearities in the APS lend themselves specifically to detecting small changes in morphology and density.

2.3. DRUM Sampler

[13] The second dust size measurement instrument was the eight-stage Davis Rotating-drum Universal size-cut Monitoring (DRUM) impactor from the University of California, Davis [Cahill *et al.*, 1985] that was collocated with the filters and APS. The DRUM was in operation for only the second, more intensive half of the study (1–30 September). Samples were collected on Apiezon grease coated strips with nominal 4-h resolution, but functionally 8–12 h. 50% diameter cut points were at $5\text{ }\mu\text{m}$, $2.5\text{ }\mu\text{m}$, $1.1\text{ }\mu\text{m}$,

0.74 μm , 0.56 μm , 0.34 μm , 0.24 μm , and 0.07 μm . The DRUM was slightly modified from that used by Reid et al. [2003] to improve performance. Flow rate was increased to 16 l min⁻¹, and the inlet tapped off of the common inlet, thus preventing the inlet losses described by Reid et al. [2003]. Sample strips were subjected to XRF analysis at the Advanced Light Source of Lawrence Berkeley National Laboratory to measure elements Al through Cu. Analysis of elemental data is given by Reid et al. (manuscript in preparation, 2008). As in the filter samples, we use the mass distribution of Fe and Ca.

[14] Like the APS, impactors have their own set of sampling issues, most notably bounce-off and potentially shatter of aggregates from upper stages onto lower stages (most during high-concentration events).

2.4. Sun-Sky Retrievals

[15] As part of the UAE² study, the Aerosol Robotic Network (AERONET [Holben et al., 1998]) deployed the densest mesonet of Sun-sky scanning radiometers in the history of its program. Here we utilize the AERONET new version (ver. 2 [Dubovik et al., 2006]) of the original Sun-sky retrievals described by Dubovik and King [2000]. Included are retrieved volume distributions, indices of refraction, single scattering albedo, and asymmetry parameter at 440, 675, 870, and 1020 nm. For a complete description of the AERONET contribution to UAE² and the new retrieval, and descriptions of regional retrieved optical properties see Eck et al. [2008].

[16] While the version 2 retrieval is a marked improvement, we are nonetheless cautious with its application. Because southwest Asia is a highly heterogeneous environment it can be difficult to derive a proper retrieval of “pure dust.” Consider the retrieval provides an “average” index of refraction between the fine (pollution) and coarse (dust) modes. For consistency, we only employ retrievals where the midvisible angstrom exponent was <0.4. Additionally all analyzed retrievals correspond to 440 nm optical depths above 0.4.

2.5. Other Data

[17] In our analysis of dust sources, we also utilized a variety of aerosol transport models and tools. Much of our meteorological analysis is drawn from Walker et al. (manuscript in preparation, 2008) including analysis from mesoscale models and 52 UAE weather stations. Regionally synoptic observations from airports (including Abu Dhabi, Dubai, Al Ain, Fujairah, Bahrain, Kuwait, and Baghdad) were used. Back trajectories were made using the NOAA Hybrid Single-Particle Lagrangian Integrated Trajectory system [Draxler and Hess, 1997].

3. Results: Grouping of Dust Properties

[18] A complete time series and chemical analysis of aerosol properties taken at the MAARCO site can be found in a number of manuscripts from the UAE² study, including Reid et al. (manuscript in preparation, 2008) for dust, K. E. Ross et al. (Fine mode aerosol particles in the southern Arabian Gulf and United Arab Emirates, manuscript in preparation, 2008) for fine mode particles, Walker et al. (manuscript in preparation, 2008) on meteorology, and J. S.

Reid et al. [2008] on aerosol-meteorology coupling. Important periods are summarized in Figure 1.

[19] Figure 1a presents a mission time series of 24-h PM_{2.5} and PM_{2.5} to inlet (i.e., regulatory defined fine and coarse mode, respectively) filter data as well as derived total dust and pollution dry mass concentrations via the receptor analyses of Reid et al. (manuscript in preparation, 2008) and Ross et al. (manuscript in preparation, 2008), respectively. Average dust and pollution concentrations were 125 ± 75 and $30 \pm 10 \mu\text{g m}^{-3}$, respectively. Average 500 nm optical depth at MAARCO was $\sim 0.5 \pm 0.1$ with a fine mode fraction of 0.4 ± 0.1 [Eck et al., 2008].

[20] The 24-h samples, while showing the influence of eight major dust events, do mask important fine features of dust transport in the region. Figure 1b shows proxies for airborne dust and sulfate (the primary pollution species, as found by Ross et al. (manuscript in preparation, 2008)) derived from hourly APS data. Here we simply integrated the volume based on aerodynamic diameter between 0.8 and 10 μm to identify coarse mode dust. The smallest APS channels were also sensitive to pollution concentration and for demonstration purposes we use the aerodynamic volume of the 0.542 μm channel as a qualitative proxy for pollution. From Figure 1b, the fine-scale nature of the events becomes clear. Between 11 August and 2 October, the APS observed 16 peaks with concentrations above $200 \mu\text{m}^3 \text{ cm}^{-3}$ (1 sigma). Large events as perceived by the filter data are in reality a number of smaller events, such as in the period between 22 and 28 August. Besides the synoptic-scale features associated with large-scale shifts in the region, a very strong diurnal cycle associated with the sea/land breeze often appeared as described by Zhu and Atkinson [2004] and Eager et al. [2008]. During the day, a sea breeze brought dust from the gulf into the interior of the UAE. Conversely, a spike in dust concentration often occurred for a 3-h period around $\sim 0400\text{--}0800$ local time as dust that had accumulated the day before in the interior was released into the Arabian Gulf by the offshore land breeze. Consequently, interior dust was a combination of local UAE dust and dust from long-range transport brought into the UAE by the onshore afternoon sea breeze the previous day. Also at times, strong nighttime offshore winds lifted dust along the coast.

3.1. Bulk Nature of Aerodynamic Size Distribution

[21] We begin our analysis by examining the aerodynamic size distribution of all 50 24-h average sample periods taken during the study. Each distribution is matched with the ~ 0900 LST initiated filter samples (e.g., 0900 to 0900 LST the following day). Volume, area, and number distributions are presented in Figures 2a, 2b, and 2c, respectively. The volume and area are computed on the basis of indicated aerodynamic diameter (d_{aei} , the raw aerodynamic diameter assigned by the APS with no additional corrections). Each 24-h average distribution was normalized by the total coarse/common mode volume ($0.8 \mu\text{m} < d_{\text{aei}} < 10 \mu\text{m}$). Hence, area and number distributions have units of “per unit volume.” While these are 24-h samples, the nature of the distribution was similar for hourly samples as well, even for the most severe and short-term dust events.

[22] Beginning with the volume distribution (Figure 2a), we see some day-to-day variance in distribution shape and

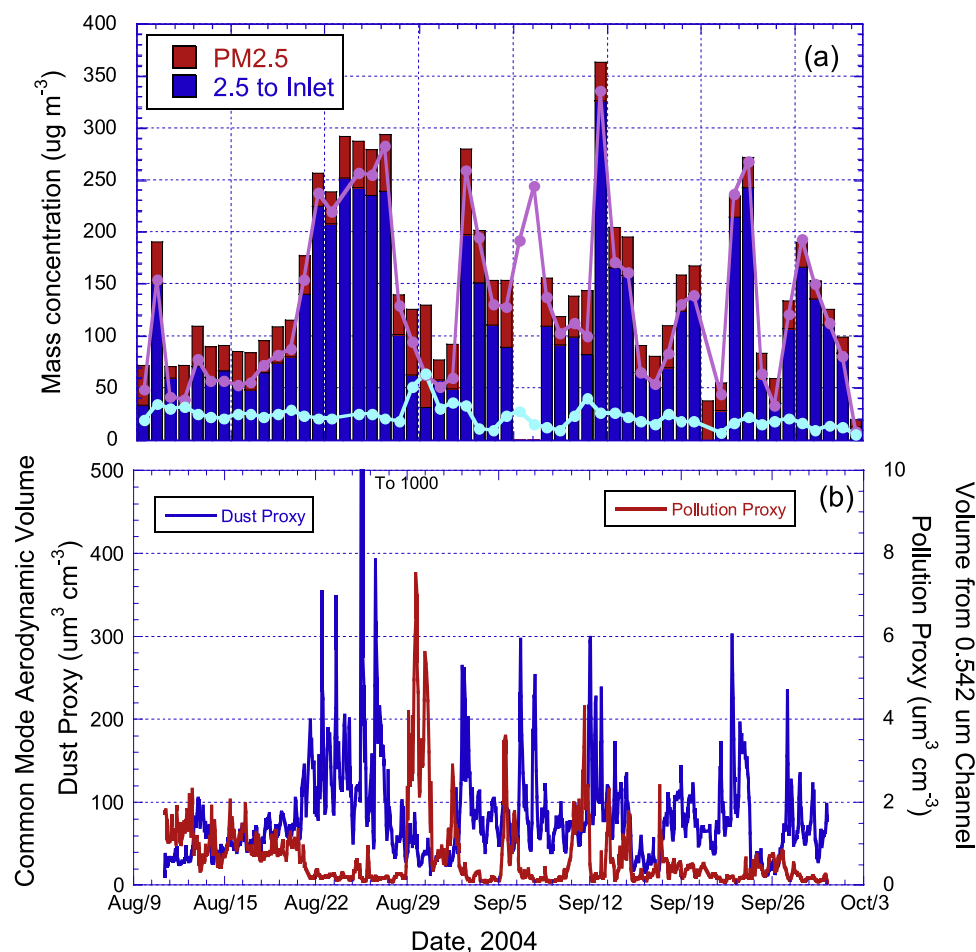


Figure 1. Time series of filter and APS 3321 data at the MAARCO site. (a) Teflon filter data showing $\text{PM}_{2.5}$ (red) and 2.5 to $\sim 15 \mu\text{m}$ (e.g., coarse) diameter particle mass. Also shown are the derived dust (purple) and pollution (light blue) mass concentrations based on the analysis of E. A. Reid et al. (manuscript in preparation, 2008) and Ross et al. (manuscript in preparation, 2008). (b) Hourly APS 3321 data. Given are the volume of the dust common mode ($\sim 0.80\text{--}10 \mu\text{m}$) based on aerodynamic diameter as a proxy for dust and the volume from channel 2 ($0.542 \mu\text{m}$ endpoint) which was found to be a good proxy for sulfate for the study period.

size. On the basis of lognormal curve fits, indicated aerodynamic volume median diameter (VMD_{iac}) ranged from $\sim 3\text{--}5 \mu\text{m}$ with geometric standard deviation (σ_{gvi}) on the order of 1.7–2.2. Given the proximity to the source region we might expect a higher concentration of giant particles ($d_{\text{aci}} > 10 \mu\text{m}$). We suspect the perceived falloff in larger sizes may be in part a sampling issue due to an inlet/plumbing cut point to the APS on the order of $10 \mu\text{m}$ diameter. However, given the common mode is $\sim 5 \mu\text{m}$, the falloff should not impact our analysis here.

[23] The volume distributions are roughly lognormal, but with a positive skewness due to a falloff for particles $d_{\text{aci}} > 7 \mu\text{m}$. Consequently, modal diameters are slightly larger than median diameters. Contributions to the overall volume distribution by smaller modes are visible with varying weights on each day. The most dominant has a $6 \mu\text{m}$ mode, with a less dominant mode at $\sim 3.5 \mu\text{m}$. The impact of pollution is also visible at times with the upswing in particle volume for $d_{\text{aci}} < 0.8 \mu\text{m}$.

[24] In the area distribution (Figure 2b), the various components of the common dust mode are more clear at 3.5 and $2.0 \mu\text{m}$. While small in total volume the $\sim 2 \mu\text{m}$ mode can have a more significant contribution to the area distribution. The ratio of area to volume (important for a host of geophysical parameters such as optics, chemistry, and geophysics) only varied by $\sim 20\%$. At times the submicron pollution mode is also visible in the area distribution ($d_{\text{aci}} < 0.8$). In the number distribution (Figure 2c), from $2 \mu\text{m}$ and greater, the distributions look very similar, and a juncture point exists at $3.5 \mu\text{m}$. Count median diameters (CMD_{aci}) appear to be in the 0.9 to $1.3 \mu\text{m}$ range.

3.2. Classification of Dust Size Distributions

[25] In an effort to understand the nature of dust size during the UAE² mission, the first step was to search for commonalities. While the original analysis utilized a number of unsupervised statistical methods (factor, cluster, multivariate, etc.), no clear patterns were obvious. Only once a hand analysis was performed initially through segregation of size ratios between the modes in Figures 2a

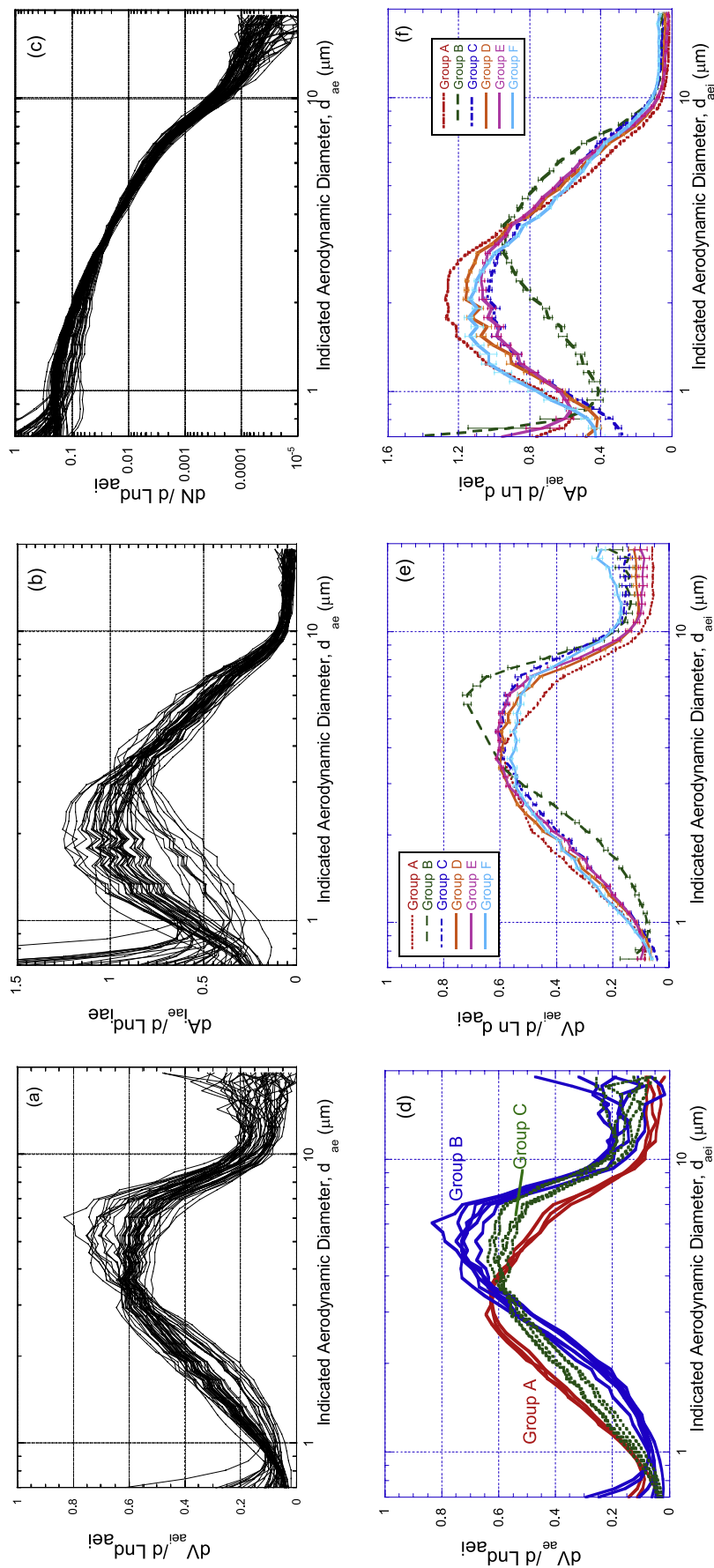


Figure 2. Volume normalized indicated aerodynamic size distributions from the MAARCO APS 3321. Given are the daily averaged (a) volume, (b) surface area, and (c) number distributions. (d) Same as Figure 2a for three sets of distributions of similar shape. Groups B and C show every other distribution. (e and f) Averaged volume and area distributions that fit into six shape groups found in the data set. Error bars show standard error for each distribution. Each curve is normalized by each's own aerodynamic dust common mode volume (e.g., $V = (\pi/6)d_{ae}^3$), taken to between $0.8 < d_{ae} < 10 \mu\text{m}$.

Table 1. Measured Properties of Coarse Mode Dust Particles Measured at MAARCO^a

	Group A	Group B	Group C	Group D	Group E	Group F
Strength/confidence	very strong	very strong	strong	moderate	moderate	moderate
Dates in August	13, 14	11, 12, 15, 30, 31	22–28	–	16–21, 29	–
Dates in September	23	1, 12, 15, 16, 25, 26	2, 7, 8	5, 13, 14, 17–22	11, 20, 24, 27, 28	3, 4, 6, 9, 10, 29
Source	NW UAE sand and gravel fields	Iraq, Tigris/Euphrates	interior Arabian Peninsula, Yemen	S. UAE sand/gravel fields	interior UAE	interior UAE
APS (based on d_{aei})						
VMD (μm): σ_{gv}	3.25::1.93	4.56::1.78	4.00::2.06	3.60::1.96	3.77::1.95	3.72::2.18
AMD (μm): σ_{ga}	2.05::1.99	2.96::2.05	2.20::2.27	2.19::2.05	2.22::2.11	2.19::2.23
Average χ_{as}	2.4	2.2	1.65	2.6	1.7	2.35
Indicator Elements	–	Pb, Va	Ca	–	–	Al
Al/Fe	2.1 \pm 0.1	2.1 \pm 0.1	2.0 \pm 0.8	1.9 \pm 0.2	2.1 \pm 0.2	(1.8 \pm 0.3)
K/Fe	0.51 \pm 0.07	<0.53 \pm 0.05>	0.46 \pm 0.05	0.47 \pm 0.03	0.49 \pm 0.04	0.47 \pm 0.04
Ca/Fe	(4.0 \pm 0.35)	4.5 \pm 0.8	<8.9 \pm 1.3>	5.0 \pm 0.9	4.2 \pm 0.7	5.8 \pm 0.8
Zn/Fe	0.011 \pm 0.003	<0.019 \pm 0.007>	(0.008 \pm 0.002)	0.012 \pm 0.003	0.012 \pm 0.005	0.009 \pm 0.001
Pb/Fe	0.004 \pm 0.002	<0.011 \pm 0.006>	0.002 \pm 0.001	0.003 \pm 0.002	0.005 \pm 0.002	0.003 \pm 0.001
DRUM (based on d_{ae})						
Fe d_{ae} MMD (μm)	3.7	5.1 \pm 0.5	4.2 \pm 0.1	4.3 \pm 0.1	4.5 \pm 0.1	4.4 \pm 0.3
Ca d_{ae} MMD (μm)	4.2	5.4 \pm 0.7	4.2 \pm 0.1	4.7 \pm 0.2	5.0 \pm 0.3	4.6 \pm 0.3
AERONET (optical equivalent)						
VMD (μm)	4.1	6.0 \pm 0.6	4.4 \pm 0.4	4.2 \pm 0.1	4.6 \pm 0.2	4.7 \pm 0.1

^aIncluded is confidence in robustness of group, dates in August and September the groups were observed, and likely source region. Parameters include size parameters from the APS based on indicated aerodynamic diameter and estimated non-Stokesian dynamic shape factor based on comparisons of coincident filter mass (χ_{as}). Key indicator elemental ratios to Fe are given, with statistically <high> and (low) ratios given. Mass median diameters (MMD) for the key soil elements of Fe and Ca for the DRUM impactor (September only) are also presented. Lastly, retrieved optical equivalent diameters based on AERONET Sun/sky retrievals are given.

and 2b, did it become apparent that there were a number of separate distribution shapes with at times degenerate simple lognormal parameters. The hand analysis resulted in three very distinct groups, labeled A, B, and C. As an example of how we defined differences in distribution shape, 24-h samples for these groups are presented in Figure 2d (all three samples for group A are presented, and every other sample for groups B and C). We also isolated an additional three groups, D, E, and F, that while similar in shape, had statistically significant different perturbations in volume or area distribution. Normalized mean volume and area distributions for all six groups are presented in Figures 2e and 2f, respectively, and physical details derived utilized in our analysis are in Table 1. Included in Figures 2e and 2f are standard errors for each group which are in some cases so narrow they do not even extend past the thickness of the line.

[26] Groups A and B reflect the two extremes in size. Group A, with the smallest volume modal diameter (3.3 μm), consisted of daily samples from 13 and 14 August and 23 September. Despite these samples being more than a month apart, their daily average size distributions are nearly identical. Conversely, for the largest sized particles in group B (11, 12, 15, 30, and 31 August; 1, 12, 15, 16, 25, and 26 September) the 6 μm volume mode is dominant whereas the 3 μm mode is much more subdued.

[27] Between groups A and B we can examine the total range of possible observed sizes. Indicated aerodynamic volume modes range from 3.3 to 6.0 μm (a factor of 1.8), similar in fraction to the ratio of surface area modes of 2.0 to 3.3 μm (a factor 1.65). Despite the large size differences, these cases have integrated aerodynamic surface area to volume ratios ranging from 2.1 to 1.7, or only 24% variance. Such variability in the result is an indication that the impacts of the raw distributions are only semilognormal (as we would expect a factor of 1.8).

[28] To explore size distribution variability and shape issue further, lognormal fits were made to each of the distributions as well as the group means (given the small standard errors in the mean, there was no significant difference). For groups A and B, VMD_{aei} values ranged from 3.25 to 4.56 μm (40% increase) with σ_{gvi} from 1.78 to 1.93. While fits had high r values (0.95–0.99) they did have difficulty representing the rapid falloff on the right side of the distributions. Consequently, best fit VMD_{aei} values do not necessarily correspond with modal diameters, as would be expected in a truly lognormal distribution. For group A, the most lognormal of distributions, the difference between volume median and mode is fairly negligible. For group B the difference is over 30%.

[29] Curve fits for area distributions are considerably more lognormal than their volume counterparts with all fits being excellent ($r > 0.99$). Modal and AMD_{aei} are within 5% ranging from 2.04 for group A to 2.96 for group B. The apparent dichotomy between the behavior in volume and area distributions serves as a warning as to the complexity of dealing with parameters that are dependent on different distribution moments. Even so, the best fit area to volume ratio does not vary significantly from the integrated values.

[30] Our third unique population, group C, has size characteristics between groups A and B with what appears to be equal contributions from the 3.5 and 6.0 μm components. Like other groups, it too has events that occurred over

a long time period (22–28 August; 2 and 8 September). One of group C's distinctions, however, is its wide geometric standard deviation (2.06 and 2.27 for the volume and area distributions, respectively).

[31] The three less distinct groups, D, E, and F, account for just over half of the samples. Because these groups have similar size characteristics, they could be lumped into one group. However, they do have statistically significant differences from each other, as well as from groups A, B, and C.

3.3. Filter Data

[32] It is important to reiterate that the group classifications described in section 3.2 were based purely on the APS indicated size distributions alone without any supporting evidence. Only once each sample was classified did we look for factors that joined group members together including filter elemental chemistry and mass. As discussed by Reid et al. (manuscript in preparation, 2008), most key soil elements for all filters correlated well with one another, with clays and silicate elements Al, Si, Ti, Fe, and Cr being most tightly related (e.g., Al:Si:Fe = 2.1:7.25:1). The strongest separator was found in Ca, an indicator of carbonates or, less likely, plagioclase feldspars or sodium calcium aluminosilicates. Interestingly, our three primary groups had strong clustering within a plot of VMD_{aei} and the Ca:Fe ratio (Figure 3a), with group C having a near factor of two enrichment in Ca, and group A being slightly lower than the others. In addition to the VMD_{aei} to Ca:Fe clustering to further isolate groups C and A, notable perturbations in trace elements between the groups included: in group B, Pb and Va were highly enriched (factor of ten and two, respectively), and K was slightly enriched (10%); and group F was the only group that statistically deviated from the Al:Fe ratio with a 10% reduction in Al.

[33] If we closed our analysis here, we would almost certainly combine groups D and E, and exchange some members with group F (if not entirely include F). But by including total mass data, such a consolidation may be a mistake. The ratio of integrated volume to filter soil mass can be used to test for changes in morphology through integration of the equation relating aerodynamic diameter (d_{ae}):

$$\text{or } Soil\ mass = V_{ae}\rho_p\left(\frac{\rho_o\chi}{\rho_p}\right)^{3/2}, \quad (1)$$

where V_{ae} is the integrated particle volume using aerodynamic diameter, ρ_p is particle density, and χ is the dynamic shape factor, an empirical drag correction term. Soil mass and V_{ae} are measured quantities. Through their ratio we can examine the nature of density/dynamic shape factor. For ρ_p , based on the values of *Emiliani* [1987] common individual mineral species vary in density from 2.45 to 2.76 g cm⁻³, for say silicon oxide versus illite. For bulk dust, 2.5 ± 0.2 g cm⁻³ is a good approximation. Given the square root relationship, ρ_p can account for at most ~10–15% change in d_{ae} , making it a nonissue for our observed variability.

[34] While χ is a convenient concept in the Stokes regime, χ is nevertheless an ambiguous size-independent empirical correction factor. Because APS flow rates through

the inner nozzle are high, χ needs to be increased to account for the instrument's non-Stokesian flow conditions (χ_{ns}). By nature, χ_{ns} in an APS can be large, and particle size and density-dependent (increasing asymmetry results in undersizing, and increasing density results in oversizing; e.g., *Marshall et al.* [1991] and *Cheng et al.* [1993]). For unit density asymmetric particles, these studies showed $\chi = 1.20$ resulted in an undersizing of factors of 25 to 70%. In comparison measured χ ranges from 1.30 to 2 for different dust species [*Davies*, 1979; *Noll et al.*, 1988], well outside the range of these laboratory studies.

[35] A consequence of particle asymmetry is that even minor changes in bulk χ values for particles could be dramatically amplified in the APS, particularly for higher moment distributions such as volume. We can use the nature of the APS to our advantage to test for changes in particle morphology by modifying equation (1):

$$Soil\ mass = V_{aei}\rho_p\left(\frac{\rho_o\chi_{ns}}{\rho_p}\right)^{3/2} \Rightarrow \chi_{ns} = \frac{\rho_p^{1/3}}{\rho_o}\left(\frac{Soil\ mass}{V_{aei}}\right)^{2/3}. \quad (2)$$

Plots of integrated common mode volume from APS indicated aerodynamic diameter versus Reid et al.'s (manuscript in preparation, 2008) reconstructed soil mass are presented in Figure 3b. Most of the dust groups follow similar patterns, with A, B, E, and F having reasonably strong regressions (0.91 < r < 1) with slopes of 0.41 to 0.58. Group D also has a strong regression (r = 0.86) although with a fairly low slope compared to others (0.27). Unlike the other groups, group C shows no particular pattern; while the derived slope is similar to the others (0.45), the uncertainties are large and the absolute magnitude is far and away the largest, with a mean value of 0.72. If we combine all data except group C into one regression, we derive a slope of 0.43 and r = 0.93. Interestingly, groups A, B, E, and F all have higher correlations than the unified regression. Overall, Figure 3b suggests a factor of 2 variation in the indicated volume to mass ratio (or 2.6 depending on how group C is treated). Using equation (2) and assuming $\rho_p = 2.5$ g cm⁻³, we derive fairly unique χ_{ns} values of 2.4, 2.3, 1.6, 2.6, 1.7, and 2.3 for A through F, respectively.

[36] Ultimately, combining chemical and morphological analysis of filter data leads us to the first conclusion that samples within groups are probably unified by source region, rather than by some atmospheric process or specific instrument bias. Further, while there is clear separation in particle chemistry and morphology, these parameters are not the overarching causal factors in the size characteristics of the six groups.

3.4. Substantiating Size Information

[37] While the above analyses indicate that the groups defined by size have unique chemical and morphological features, the nature of the APS measurement process leads to significant uncertainty as to what the actual size of the dust particles is. To investigate, we compared APS data to two other coarse mode measurement techniques, the DRUM cascade impactor and Sun/sky retrievals from AERONET Sun-sky radiometers. While each of these methods has its own distinct sampling and measurement issues (see *Reid et*

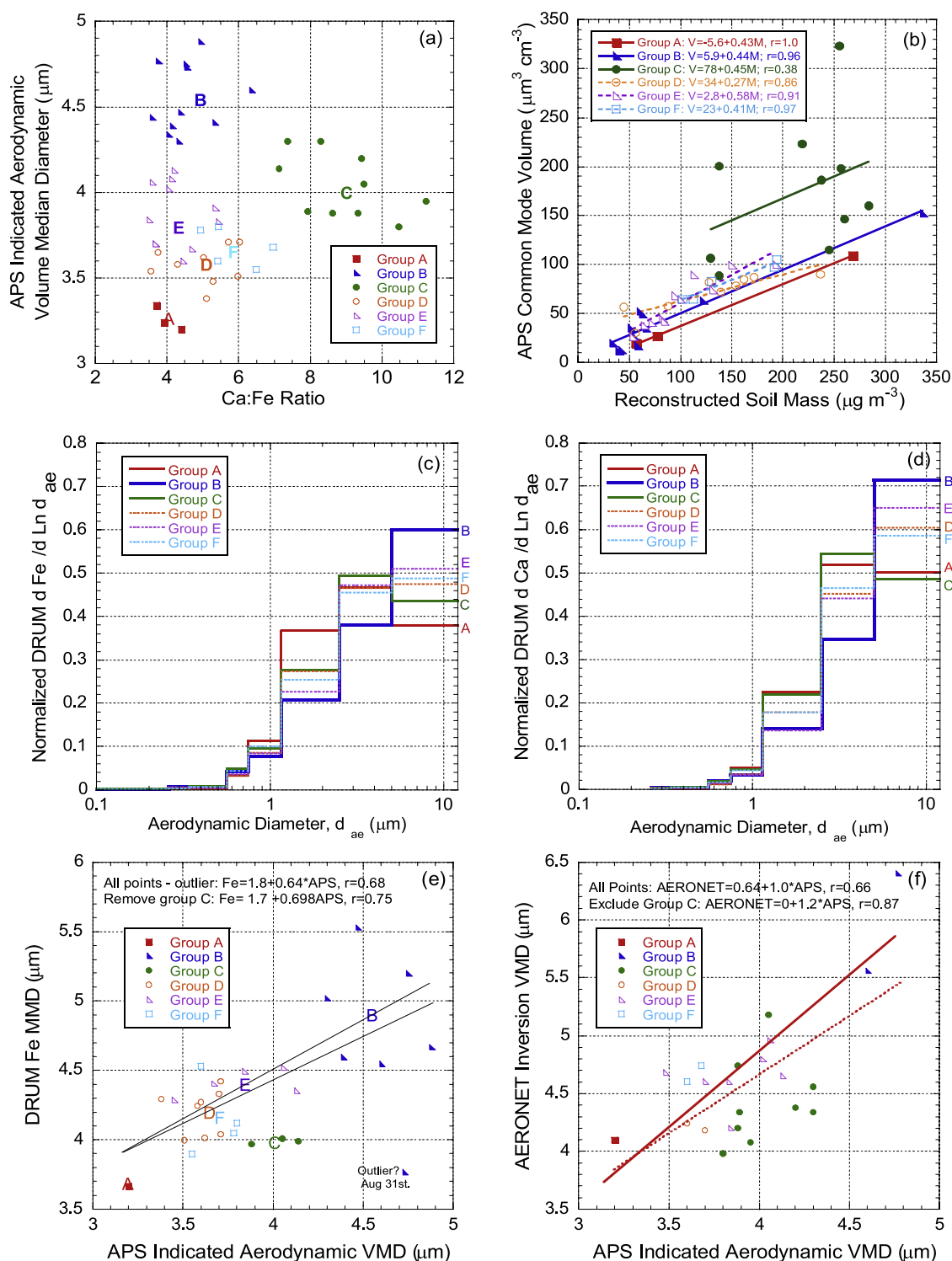


Figure 3. (a) The 24-h average APS distribution indicated aerodynamic VMD as a function of TSP calcium to iron ratio. The mean value for each group is listed as a bold letter. (b) The 24-h average common mode regressions of APS common mode versus TSP mass. (c and d) DRUM impactor Fe and Ca mass distributions. (e) DRUM Fe MMD versus APS indicated aerodynamic VMD. (f) Retrieved AERONET MMD versus APS indicated aerodynamic VMD.

al. [2003] for details), the DRUM and retrievals substantiated findings from the APS.

[38] Overall, the DRUM Fe and Ca distributions are consistent with the APS (Figures 3c and 3d, respectively).

Qualitatively, Fe and Ca sizes correlate, but with a clear propensity for soil elements associated with Ca being larger than those with Fe, by ~ 10 – 30% . Overall, 90% of the soil mass is $>1 \mu\text{m}$ and no discernable submicron mode.

[39] Like the APS, group A clearly has the smallest distribution, with a mode in stage 2 (2.5–5 μm), and a sizable mass fraction in stage 3 (1.15–2.4 μm). Similarly, group B is the largest, with group C in between. Overall, qualitative sizing of the APS appears to be consistent between most groups with stage 1 mass fractions going as $A < D < F < E < B$, the same order as APS VMD. Thus, with again the exception of group C, which is clearly out of place, the size trends between the APS and DRUM are consistent. To be more quantitative, we plotted Fe and Ca MMD with the APS VMD by group (Figure 3e). Because most mass is in the top three stages with significant mass contributions from stage 1, uncertainties in computed MMD can be large. But generally, correlations track our impressions of Figures 3c and 3d. The one clear outlier sample was associated with the group B 31 August sample. For 31 August, concentrations were very low with significant relative background submicron soil component, driving down the MMD.

[40] Considering dust mass is mostly in Fe-related species, we expect the overall DRUM MMD to be weighted heavily by the Fe distribution. Knowing that the DRUM sampler slightly underestimates size because of such issues as bounce-off, and from the χ_{ns} values derived in the previous section, we would expect that the APS is under-sizing on the order of 5–20% in diameter, or 15–60% in volume. These sizing underestimates are satisfying in that the APS is performing as predicted from previous calibration studies, and is within the range for larger χ values for dust independently derived by Davies [1979] and Noll *et al.* [1988] (χ approx 1.5–1.7).

[41] In addition to the impactor, we can perform some rudimentary comparisons to AERONET Sun/sky retrievals. Such a comparison is even more difficult, in that we are comparing a surface site to a vertical integral. Do to size retrieval errors in heterogeneous coarse-fine mixtures we only used retrievals where the atmosphere was dust-dominated (angstrom exponent < 0.4); a constraint that removed more than 80% of the retrievals, including nearly all of those at the MAARCO site. But for completeness, on each day we did average all available regional data. The dominant contributor was the Hamim site, some 200 km to the southwest of MAARCO, although other closer sites contributed. While comparison between sites of such distance is by no mean ideal, most of the dust events were regional in nature and for intensive properties such as size, there should be some correlation between the APS and AERONET. A plot of these data is shown in Figure 3f.

[42] In general, the inversions demonstrated the same patterns as the DRUM sampler with an overall r value of 0.66. Groups A and B are at the far sides of the regression, and group C is conspicuously low biased. Removing group C from the regression substantially increases r to 0.87. But overall, the comparison gives further evidence that the shifts in size observed by the APS are actually related to true particle size.

3.5. Source Region Identification and Transport

[43] Thus far our analysis points to the conclusion that for at least three groups (and potentially three more) the dust sampled at the MAARCO site comes from specific sources (through elemental chemistry and morphology) and/or has

been similarly modified in shape because of transport processes (through size). No “causal” factors for either have yet been determined. In section 3.5 we examine whether the meteorology and transport phenomena of members of these groups have any consistencies. There is strong observational evidence during the mission suggesting the source of several of the largest events making up groups A, B, and C, and allowing intelligent speculation on the remaining sources. These are all discussed in detail by Walker *et al.* (manuscript in preparation, 2008) and *J. S. Reid et al.* [2008]. Each case is described separately here in order of certainty.

3.5.1. Group B: Iraq

[44] Our easiest source region to identify is for group B. One of the largest events of the UAE² campaign occurred on 12 September 2004, when a large dust event originating in Iraqi Tigris-Euphrates Valley was transported south across the Arabian Gulf into the UAE. Ample satellite data allowed us to follow the plume’s development in the region and its impact at the MAARCO site. Examination of the transport meteorology for all group B members indicates a point of origin in the Tigris/Euphrates valley [*J. S. Reid et al.*, 2008]. HYSPLIT back trajectories suggest all members of group B show similar trajectories from the northern Arabian Gulf and Iraq (Figure 4a). Such trajectories explain the unique chemical signature of group B, particularly the enrichment of Pb in chemistry samples with likely sources in the regional petrochemical flaring.

[45] Despite the similarities in dust size in group B, the amount of time these measured air parcels spent in the Arabian Gulf marine boundary layer varied significantly. First, peaks in dust concentration varied in altitude daily from MBL dominated, to just above the MBL inversion [*J. S. Reid et al.*, 2008]. In a third of the cases, the southwesterly monsoon was so strong that it overshadowed any sea breeze development (15 August; 12, 15, and 16 September). Not only was the transport time short, but dust concentrations were among the highest measured during the study. For the 12 September event, which first gave us an indication of the source, production was related to $12 + \text{m s}^{-1}$ wind speeds recorded at the surface in Iraq with widespread visibility reduction to < 2 km. A middle set of cases required 2 to 5 days to reach the UAE (11 and 12 August; 25 and 26 September). The last subgroup (30 and 31 August; 1 September) was from a stagnation event over the northern Arabian Gulf in which, on the basis of both satellite and back trajectory analyses, the air mass was trapped in the Arabian Gulf for more than 4 to 5 days. Production winds in Iraq preceding the middle and long-term transport events never reached more than 8 m s^{-1} and were accompanied by only moderate visibility reduction. Further, while these stagnation cases held some of the highest 24-h sulfate concentrations for the study, they also had the lowest dust concentrations.

3.5.2. Group C: Oman and Yemen

[46] Group C events were all associated with strong offshore flow that overpowered any land/sea breeze. During the period 22–28 August, a strong heat low developed over Saudi Arabia and simultaneously the Indian monsoon weakened, causing the winds to become southwesterly [*J. S. Reid et al.*, 2008; Walker *et al.*, manuscript in preparation, 2008]. Back trajectories for the 28–28 August time

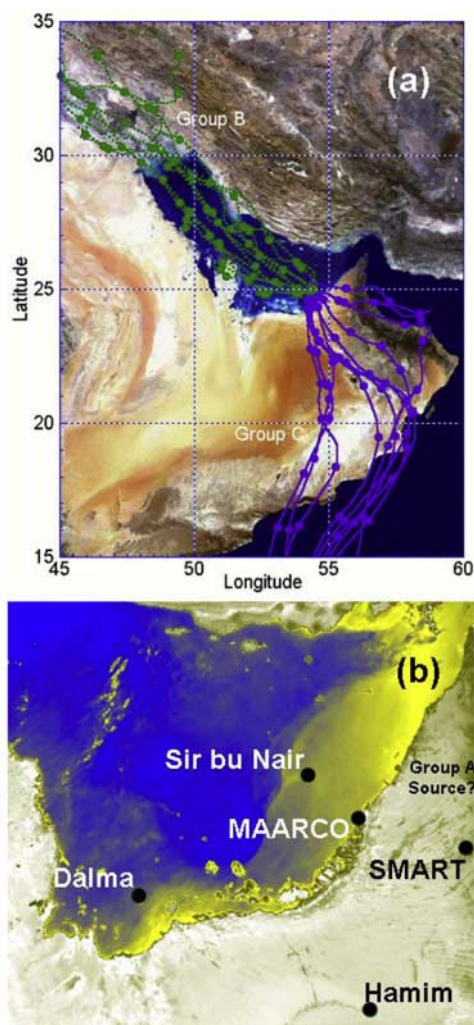


Figure 4. (a) READY HYSPLIT back trajectories from the MAARCO site for dust particle size groups B (green) and C (purple). Background image from a regional MISR composite (courtesy of Jim Knighton, Glendale College, California). (b) AATSR enhancement of dust plume off of the UAE coast for the 23 September 2004 dust event in group A (image courtesy Robin Schoemaker, TNO, Netherlands). Included are the locations of AERONET sites with similar size and index of refraction retrievals.

period were consistent, with air masses moving from southern Oman and northern Yemen into the UAE (Figure 4a). Optical depths between MAARCO and the interior desert sites were correlated well, thus indicating large-scale dust coverage. Most trajectories pass near the limestone and salt-rich gravel beds of Yemen identifiable by the white region on the image (Reid et al., manuscript in preparation, 2008), possibly accounting for some of the higher Ca concentrations.

[47] While the synoptic forcing was not as strong for 2, 7, and 8 September, the pattern and end result was the same. Complicating the situation, however, is that for 7 and 8 September, there were also individual plumes visible emanating from coastal UAE sources, which also tend to be carbonate rich. Such colinearity between long-range transport and coincident local production may explain some

of the chaotic nature of group C; although no systematic pattern with regards to the filter data was visible to us, distribution shapes and Ca:Fe ratios are the same. Because the DRUM did not run in the first part of the study, we cannot compare its size to the APS for the August versus September events. But AERONET retrievals did differ systematically across the region. In Figure 3f, the two highest data points along the regression line were in fact associated with the 7 and 8 September events and were from the Sir Bu Nair island site some 50 km offshore of MAARCO, potentially indicating a different source. Further, Sun/sky retrievals between the interior and coastal AERONET sites for absorption were similar, but statistically different in retrieved index of refraction which varied from 1.48 in the interior to 1.52 on the coast. Optical depths at the coast were also slightly higher (0.49 versus 0.41 at 440 nm). So clearly, there is some contamination. But the reaction of the APS with regard to particle shape was the same, possibly indicating a specific mineralogy or soil morphology component to the APS's response function. Ultimately, we surmise that for the 7 and 8 September cases there is some local contributions in the signal which may account for the scatter in group C results.

3.5.3. Group A: UAE Sand Fields

[48] During group A's three events, poor visibility was reported in a region spanning from Bandar Abbas, Iran, north of the Strait of Hormuz, through the northern half of the UAE. The strongest of these events occurred on 23 September (Figure 4b) and AERONET retrievals of size and index of refraction over the southern UAE were similar ($4.0 \mu\text{m}$ VMD, index of refraction $1.48-0.003i$ at 440 nm). The pattern of surface reports for the group was fairly unique during the mission. Unlike group B, mesoscale flows dominated the region, with the mesoscale model flows from COAMPS[®] and observations being at odds with the synoptic models. On the basis of surface observations and geostationary satellite image time series, during a period of very light winds and little synoptic forcing, dust appears to be looping through the UAE into the Arabian Gulf and Strait of Hormuz from the northern UAE. While the morning land breeze brought the dust out over the water, the afternoon sea breeze brought it back into the UAE, ultimately resulting in a 12-h time period in which the size distribution of dust was stable and strictly conformed to the daily averaged group A shapes. A similar flow pattern was observed for the 13 and 14 August cases as well, resulting in a lower concentration but again remarkably stable size distribution for 28 h. The attribution of group A to the northern UAE region is consistent with the elemental chemistry as it is dominated by sands and is Ca poor (Reid et al., manuscript in preparation, 2008).

3.5.4. Groups D, E, and F: Miscellaneous Regional Sources

[49] One of the difficulties in analyzing data in the Arabian Gulf is that under most circumstances, regional synoptic flows are perturbed by the very strong mesoscale and sea breeze flows that form along the coast [Zhu and Atkinson, 2004; Eager et al., 2008]. In the case of groups D, E, and F, flow patterns in the region suggest that these cases were heavily influenced by such mechanisms. The interplay of the offshore morning land breeze and the onshore afternoon sea breeze creates a number of individual dust

fronts and plumes from a variety of sources with events lasting hours to a day.

[50] All the sources of groups D, E, and F appear “local” in nature and likely are dominated by sources within or near to the UAE. The landscape is varying with areas of large dunes, evaporate flats, and many soil types scattered over the country (Reid et al., manuscript in preparation, 2008). Dust production for these cases is likely enhanced by mesoscale events such as strong coastal wind phenomena (Walker et al., manuscript in preparation, 2008) and down-slope winds or thunderstorm outflow (or haboobs [see Miller et al., 2008]). Further, daily sea breezes are strong enough to generate dust far into the interior. Dust accumulates there, only to be released into the Arabian Gulf during early morning land breeze events.

4. Discussion

[51] The UAE² mission and the study reported here were specifically designed to examine dust variability. The location of the mission guaranteed that we would observe dust from a number of sources and transport distances with a consistent instrumentation set. Key to analysis presented here was the APS. Despite systematic sizing errors in the APS, it is one of the few commercially available coarse mode aerosol sizers with high sizing precision. Other advantages include good temporal resolution, and a lack of concentration-dependent bias. We showed that shifts in APS size track with other instruments and has semiquantitative sizing skill. It is for these reasons that the APS is one of the most commonly used instruments for dust sizing in the scientific community.

[52] Our stated goals for our work presented here included a detailed study of the causal variability in measured dust particle size distributions, and to seek verification of previous findings and ideas in the literature that dust common mode size distributions are fairly invariant for any given source or even over long transport distances [e.g., Glaccum and Prospero, 1980; Prospero, 1981; Prospero et al., 1989; Maring et al., 2003]. The issue of dust variability is independent of the question of the actual size of the dust. Indeed, dust variability in itself is an extraordinarily complicated question, and the major conclusions of Reid et al. [2003] still held at the time of our analysis. Given the variability in dust morphology, even the definition of “dust size” is ambiguous. To study dust variability it is often more direct and statistically cleaner to examine instrument data with as little processing as possible, and thus treat instrument response functions at their most fundamental level.

[53] We found that there are specific size distribution shapes that can be related to source region though the analysis of chemistry, morphology, and transport. Combination of such factors provides strong circumstantial evidence supporting previous hypotheses regarding the invariability of dust common mode size. Recall that members within each of our groups vary by less than 10% in AMD, VMD, and the accompanying geometric standard deviations. The finding of group consistency supports two primary conclusions that must be taken together: (1) The size distribution shape of common mode dust is more heavily dependent on source region soil characteristics and geochemistry than other external factors

such as production wind speed and (2) short to moderate transport distances have very little effect on the size distribution of common mode dust.

4.1. Source Influence

[54] On the basis of the dramatic daily and even hourly shifts in winds in production regions, as well as dust particle concentrations at the MAARCO receptor site, we can circumstantially infer that the common mode production size distribution is insensitive to wind speed in the area of generation. Consider Figure 1b in which hourly APS volume is plotted. Group B and C events include some of the highest and lowest hourly dust concentrations of the missions, with volume concentrations spanning over an order of magnitude. But member size distributions for each group are all very similar. Shape similarity held for even the massive case of 12 September, where production winds in Iraq were over 12 m s^{-1} [J. S. Reid et al., 2008], versus the other group cases where winds in Iraq were considerably lower. Similarly, group A has nearly identical shape distributions with concentrations that vary from $60 \mu\text{g m}^{-3}$ for 13 and 13 August to $260 \mu\text{g m}^{-3}$ for 23 September. Such amplitude shifts are probably due to a modulation of highly variable wind events over the desert (Walker et al., manuscript in preparation, 2008).

[55] The wind speed independence conclusion is similar to assumptions made in the 1970 to mid-1990s period, and is in partial agreement with more recent quantitative studies. The most comprehensive studies to date for source dust size distribution as a function of wind speed have been performed in wind tunnel tests by Alfaro et al. [1997, 1998]. These studies show that as surface friction velocity increases, there is a marked decrease in dust particle common mode VMD. Such an observation is physically plausible; as “primary” particles increase in speed during the saltation process, more energy is available to overcome binding energies of aggregates or individual minerals. However, there does appear to be a saturation point which, in the experimental design and data of Alfaro et al. [1997] appears to be on the order of friction velocity (u^*) = $50\text{--}60 \text{ cm s}^{-1}$, or roughly $8\text{--}9 \text{ m s}^{-1}$ in their wind tunnel. The observation of a “saturation point” is also reasonable, as aggregates are breaking up to individual components and/or perhaps reaching a second and much stronger level of binding energies.

[56] For typical atmospheric dust events, the maximum $u^* = 60 \text{ cm s}^{-1}$ level reached by the Alfaro et al. [1997] study are considered fairly low. For example, in the NRL Aerosol Analysis and Prediction System (NAAPS), the U.S. Navy’s operational aerosol model, dust is not even injected into the system until $u^* = 60 \text{ cm s}^{-1}$. Further, dust mass production is strongly nonlinear as $(u^*)^4$. Thus production over a large region would be dominated by the peak wind zones or even gusts and consequently favor the energy-saturated relative size distribution, hence relegating any wind speed dependence as a lower-order term. Dust particle size distribution shape would then likely be dependent on source-specific soil features such as relative sand-silt-clay mixtures, primary aggregate size, key mineralogical constituents, and perhaps moisture.

4.2. Transport

[57] Because measured size distributions are static for each source region, it necessarily follows that the transport

processes carrying common mode dust over moderate distances and times (perhaps a week or 1000 km) do not significantly impact the shape of the size distribution. For dust older than a week, certainly we expect a shift to smaller sizes. When modification does occur, it is reasonable to expect that the nonlinearities in dust scavenging mechanisms will aid in the convergence into a more uniform size [Prospero *et al.*, 1989].

[58] Expanded discussions of transport phenomena are presented by Eager *et al.* [2008], J. S. Reid *et al.* [2008], and Walker *et al.* (manuscript in preparation, 2008). Here we would like to point out two prominent examples. Group B (Iraq–Tigris/Euphrates) is of particular interest in supporting the transport invariance conclusion, because while we are confident that its members are all from the same source region, the transport times range from 1.5 days for the massive event of 11 September to over 4 days for the stagnation event of 31 August. Vertical profiles of the dust were also variable. Given that the Arabian Gulf MBL is often thermodynamically stable, the Iraqi air masses reaching MAARCO were trapped within or just above the persistent 500 m inversion (and is supported by aircraft data as well [J. S. Reid *et al.*, 2008]). The dust aloft situation should bring dry deposition into play for larger particles. Given the stable thermodynamic nature of the central Arabian Gulf, consider the settling velocity as a qualitative proxy for dry deposition (a fair assumption for low wind speeds). A $d_{ac} = 3 \mu\text{m}$ particle has a fairly small 25 m/d settling rate, small in comparison to the 500 m MBL depth. Thus, even over 4 days we expect a static distribution of smaller particles. By $d_{ac} = 6 \mu\text{m}$, the largest submode in the observed distributions, settling has increased to 100 m/d but for a stable-neutral MBL results in $\sim 15\%$ loss per day. However, for the largest particles that contribute to the giant mode, say $d_{ac} = 10$ and $15 \mu\text{m}$, settling is as high as 250 and 550 m/d, respectively, and dry deposition should be a significant physical process (or 40% and 75% per day in a neutral-mixed MBL). These high settling rates for the largest particles could explain why few dust particles were observed with $d_{ac} > 10 \mu\text{m}$, although plumbing issues likely contribute as well.

[59] In reality, dry deposition losses for the common mode should be even less evident because there is mechanical mixing and buoyant convection due to surface winds and the massive latent heat flux over the Arabian Gulf's surface [Brooks and Rogers, 2000]. Further, higher wind speeds also result in less size-dependent deposition rates. Wind speeds over the gulf are often on the order of $5\text{--}8 \text{ m s}^{-1}$, with extreme events of $\sim 10 \text{ m s}^{-1}$. Consider the dry deposition velocities predicted by the commonly used Slinn and Slinn [1980] parameterization, which yields a flattening of the deposition velocity in the $3\text{--}8 \mu\text{m}$ range for wind speeds above 8 m s^{-1} . Thus, even with significant loss to the surface, deposition may not manifest itself as a significant shift in the volume distribution shape.

[60] As a second example, consider group C from the Yemen region (August period). In almost every way, the development and transport of these air masses are the opposite of group B. Where air in group B came from over the stable Arabian Gulf, group C was transported over the interior desert. Whereas group B was transported along with a developing shallow, moist, and stable marine boundary layer,

group C was in a dry, unstable boundary layer with deep surface convection of up to several kilometers. Given the transport circumstances of group C, we expect the dust to be well mixed in the 2+ km deep planetary boundary layer during sampling. Strong dry convection would hinder observing the effects of dry deposition processes. Thus, we would expect the size distribution to remain fairly static during transport.

4.3. Implications for Global Dust Modeling

[61] There are a number of specific implications for our study. First, our results verify the findings and ideas of Glaccum and Prospero [1980], Prospero [1981], Prospero *et al.* [1989] and most importantly Maring *et al.* [2003] that dust common mode shape from any given source is fairly invariant. Given the evidence of the above studies, our conclusion are probably a fair statement for the greater Saharan desert. The implicit qualifier for dust size invariance is that it holds for those cases where the soil properties for any given source are also static, which is not always the case. Reid *et al.* [1994] did see seasonal shifts in particle size and chemistry on the Owens (dry) Lake, California, through a seasonal efflorescent crust building/depletion cycle.

[62] A second implication of our analysis is that it justifies the common practice in aerosol transport models to treat dust size distributions as static for any given source (such as Africa). Not only is size invariance a simplification for the source, but also for radiative effects, particularly in the shortwave. The qualifier here is that dust size invariance does not hold for the giant mode, which is important for ocean fertilization and possibly infrared effects (including infrared retrievals such as in the work by Pierangelo *et al.* [2005]). But if the giant mode is treated separately in the models (as it should be), it does not lessen the importance of the finding of the dynamics of the common mode.

[63] Another implication is in regards to what we did not find; we did not see evidence of a persistent submicron mode. On the basis of the APS and DRUM data, we did not see clear modal behaviors such as that suggested by Gomes *et al.* [1990] on the basis of inversions of impactor distributions, or as large as a peak as observed by Perry *et al.* [1999]. One may argue that our modes at 3.5 and $6 \mu\text{m}$ support the idea of submicron modes, but the qualitative difference is too large, in our opinion, and the possibility of bounce-off to lower stages is strongly suspect. Our findings do not prove the submicron modes do not exist, but the evidence in our data set is currently not compelling.

[64] Finally, the nature of groupings makes for an excellent starting point for further studies, particularly with regard to optical, physical, and transport phenomena. Using the strengths of the MAARCO receptor site, the UAE² mission can support a number of sensitivity studies of modeling and remote sensing systems alike.

4.4. Comparison With Other Studies

[65] On the basis of a literature survey, we found that the APS is now one of the most commonly used instruments to measure dust size, and there now exists a fairly extensive data set. Lognormal volume parameters are presented in Table 2 from key studies spanning the world's major dust producing regions, including Africa, Asia, and the United States. Given is each paper's estimation for diameter of equivalent mass (d_{em}) representation of VMD and σ_{gv} . For

Table 2. Summary of APS Derived Dust Volume Distributions for Dust Regions Over the Globe^a

	Source	Sample Location	VMD d_{aei} : Geometric Standard Deviation	VMD d_{em} : Geometric Standard Deviation
<i>Bates et al.</i> [2002]	Africa	Atlantic	3.6::1.7	2.6::1.8
<i>Bates et al.</i> [2002]	Arabian Peninsula	Arabian Sea	4.3::1.8	3.0::1.8
<i>Maring et al.</i> [2003]	Sahara	Izania, Tenerefe	4.8::2.4	3.4::2.4
<i>Maring et al.</i> [2003]		Puerto Rico	3.5::2.2	2.5::2.2
<i>Peters</i> [2006]	Phoenix	Phoenix	6.5::1.9	5.4::1.9
<i>Quinn et al.</i> [2004]	Gobi/Taklimakan	Sea of Japan	3.6::1.8	2.5::1.8
<i>Reid</i> [1993]	Owens (dry) Lake: NE	shore	5.6::~2	4.6::~2
<i>Reid</i> [1993]	Owens (dry) Lake: E	shore	3.0::1.5	2.5::1.5
<i>Reid</i> [1993]	Owens (dry) Lake: S	shore	3.9::1.6	3.2::1.6
UAE ² analysis	A: UAE sand fields	UAE coast	3.3::1.9	2.9::2.0
UAE ² analysis	B: Iraq, Tigris/Euphrates	UAE coast	4.6::1.8	4.1::1.9
UAE ² analysis	C: Yemen/Oman	UAE coast	4.0::2.1	3.5::2.2
Average			4.3::1.9	3.5::2.0
Standard deviation			1.1::0.3	1.0::0.3

^aIncluded are the dust source, the sample location, and lognormal volume parameters (volume median diameter and geometric standard deviation). Volume distributions are given on the basis of the raw aerodynamic size data (d_{aei}) and diameter of equivalent mass (d_{em}) estimation provided by the study. To convert between aerodynamic and equivalent mass based size in the UAE² data set, we used the χ_{ns} values derived in section 3.

our analysis, computations are based on the mass constraint regressions in section 3. But for a clean comparison, we also provide parameters based on the raw indicated aerodynamic data obtained from the authors.

[66] Most VMD data fits into our bound of 3–5 μm d_{aei} , or 2.5–4.5 d_{em} , with average VMD values of 4.3 ± 1.9 and 3.5 ± 2.0 , respectively. Some individual samples such as those given by *Peters* [2006] and the NE sand sheet of Owens (dry) lakebed [*Reid*, 1993] are larger by $\sim 1\text{--}2\ \mu\text{m}$, but in both of these cases, large giant modes also existed, skewing the distribution to larger sizes. But excluding these cases, the VMD for d_{em} places coarse mode dust seems to $\sim 3.5 \pm 30\%$ and a σ_{gv} of 2.

[67] What was perhaps even more interesting is that our examination of the data from these published studies revealed the exact same trends as we found in the UAE. Individual sources had remarkably similar VMD values and shapes in each study. Even in the case of *Maring et al.* [2003], which shows a shift in VMD from the coast of Africa to Puerto Rico, the shape of the coarse mode is mostly intact; the VMD shift is due mostly to a reduction in particle count in the largest sizes.

5. Conclusions

[68] Here we present our findings on the measured dust size distribution from a coastal site during the United Arab Emirates Unified Aerosol Experiment (UAE²). To be sure, the environment is complicated with a heterogeneous mix of pollution and dust from numerous sources. But using a TSI aerodynamic particle sizer, three very distinct size groups emerged, with three additional statistically significant groups also present. Groups (and possibly subgroups) had their own unique size and chemical signatures, suggesting each came from a specific source region. We surmise through meteorological analyses that these include Iraq, Yemen, and other more localized sources throughout the southern Arabian Gulf region.

[69] The UAE² data set was used as a context to study the variability of dust particle size. The actual extraction of particle sizes is complicated and will be fully described in a future paper. Our analysis presented here, however, centered on dust variability and relative changes with

source, chemistry, and meteorology. On the basis of our analysis, we came to the following conclusions.

[70] 1. Raw indicated aerodynamic dust size distributions measured by the APS were observed to vary by $\sim 40\%$ in VMD, with dust generated in Iraq having the largest sizes, and dust from the northern UAE or southeastern Iran having the smallest sizes. Variations in size parameters between groups correlated reasonably with independent DRUM impactor measurements and AERONET inversions, although clear negative size biases in the APS are visible. A strong submicron mode, proposed elsewhere, was not observed.

[71] 2. Differences in overall dust particle size in the APS for each source region were related but not correlated to particle chemistry or morphology in the APS, although in the DRUM sampler, calcium-related species (such as carbonates) appear to be $\sim 20\%$ larger than iron-bearing species (silicates, clays).

[72] 3. Similar to suggestions by *Prospero et al.* [1989] and *Maring et al.* [2003], it was found that the size characteristics of dust events were most dependent on source region, and hence appear to be dominated by source region geomorphology and roughness length rather than other external factors such as wind speed. Similarly for transport, dust events from a single source requiring up to 5 days of transport to the receptor site were nearly identical to dust arriving after only 1 day. Such an outcome greatly simplifies the source function for aerosol models that emphasize radiative effects. Even so, the relative amount of dust between the common mode and the giant mode (not studied here) is still likely to be more dynamic [*Alfaro and Gomes*, 2001].

[73] 4. When compared with the emerging global APS data set, the dust coarse mode is found to be fairly robust with rough diameter of equivalent volume or mass distributions on the order of $\sim 3.5 \pm 30\%$ μm VMD and σ_{gv} of 2.

[74] **Acknowledgments.** We would like to thank the many UAE² participants that made the MAARCO deployment successful. In particular, we would like to thank the staff of the UAE Department of Water Resource Studies, Abdulla Al Mangoosh and Sheik Monsour, for their support. We are also grateful to Tim Bates (NOAA PMEL), Hal Maring (NASA HQ), Patricia Quinn (NOAA PMEL), and Thomas Peters (University of Iowa) for providing raw APS data from their studies and to Steve Kohl (DRI) for the filter chemical analysis. We also would like to thank Dale Gillette for a helpful review of a draft version of our work. Funding was provided by the Office of Naval Research 32, Office of Naval Research 35, and the NASA Radiation Sciences Program.

References

- Alfaro, S. C., and L. Gomes (2001), Modeling mineral aerosol production by wind erosion: Emission intensities and aerosol size distributions in source areas, *J. Geophys. Res.*, **106**, 18,075–18,084, doi:10.1029/2000JD900339.
- Alfaro, S. C., A. Gaudichet, L. Gomes, and M. Maille (1997), Modeling the size distribution of a soil aerosol produced by sandblasting, *J. Geophys. Res.*, **102**, 11,239–11,249, doi:10.1029/97JD00403.
- Alfaro, S. C., A. Gaudichet, L. Gomes, and M. Maille (1998), Mineral aerosol production by wind erosion: Aerosol particle sizes and binding energies, *Geophys. Res. Lett.*, **25**, 991–994, doi:10.1029/98GL00502.
- Baron, P. A. (1996), Calibration and use of the aerodynamic particle sizer (APS 3300), *Aerosol Sci. Technol.*, **5**, 55–67.
- Bates, T. S., D. J. Coffman, D. S. Covert, and P. K. Quinn (2002), Regional marine boundary layer aerosol size distributions in the Indian, Atlantic, and Pacific Oceans: A comparison of INDOEX measurements with ACE-1, ACE-2, and Aerosols99, *J. Geophys. Res.*, **107**(D19), 8026, doi:10.1029/2001JD001174.
- Brooks, I. A., and D. P. Rogers (2000), Aircraft observations of the mean and turbulent structure of a shallow boundary layer over the Persian Gulf, *Boundary Layer Meteorol.*, **95**, 189–210, doi:10.1023/A:1002623712237.
- Cahill, T. A., C. Goodart, J. W. Nelson, R. A. Eldred, J. S. Nasstrom, and P. J. Feeny (1985), Design and evaluation of the DRUM impactor, in *Proceedings of the International Symposium on Particulate and Multi-Phase Processes*, edited by T. Ariman and T. Nejat, pp. 319–325, Hemisphere, Washington, D. C.
- Cheng, Y. S., B. T. Chen, and H. C. Yeh (1990), Behavior of isometric nonspherical aerosol-particles in the aerodynamic particle sizer, *J. Aerosol Sci.*, **21**, 701–710, doi:10.1016/0021-8502(90)90124-G.
- Cheng, Y. S., B. T. Chen, H. C. Yeh, I. A. Marshall, J. P. Mitchell, and W. D. Griffiths (1993), Behavior of compact nonspherical particles in the aerodynamic particle sizer model 33B-Ultra Stokesian drag forces, *Aerosol Sci. Technol.*, **19**, 255–267, doi:10.1080/02786829308959634.
- Davies, C. N. (1979), Particle fluid interaction, *J. Aerosol Sci.*, **10**, 477–513, doi:10.1016/0021-8502(79)90006-5.
- Draxler, R. R., and G. D. Hess (1997), Description of the Hysplit 4 modeling system, *NOAA Tech. Memo., ERL ARL-224*, 24 pp. NOAA, Silver Spring, Md.
- Dubovik, O., and M. D. King (2000), A flexible inversion algorithm for the retrieval of aerosol optical properties from Sun and sky radiance measurements, *J. Geophys. Res.*, **105**, 20,673–20,696, doi:10.1029/2000JD900282.
- Dubovik, O., et al. (2006), Application of spheroid models to account for aerosol particle nonsphericity in remote sensing of desert dust, *J. Geophys. Res.*, **111**, D11208, doi:10.1029/2005JD006619.
- Eager, R. E., S. Raman, D. L. Westphal, J. S. Reid, and A. Al Mandoos (2008), A climatological study of the sea and land breezes in the Arabian Gulf region, *J. Geophys. Res.*, doi:10.1029/2007JD009710, in press.
- Eck, T. F., et al. (2008), Spatial and temporal variability of column-integrated aerosol optical properties in the southern Arabian Gulf and United Arab Emirates in summer, *J. Geophys. Res.*, **113**, D01204, doi:10.1029/2007JD008944.
- Emiliani, C. (1987), *Dictionary of the Physical Sciences*, Oxford Univ. Press, New York.
- Gillette, D. A., and W. N. Chen (1999), Size distributions of saltating grains: An important variable in the production of suspended particles, *Earth Surf. Processes Landforms*, **24**, 449–462, doi:10.1002/(SICI)1096-9837(199905)24:5<449::AID-ESP1>3.0.CO;2-E.
- Gillette, D. A., T. C. Niemeyer, and P. J. Helm (2001), Supply-limited horizontal sand drift at an ephemerally crusted, unvegetated saline playa, *J. Geophys. Res.*, **106**, 18,085–18,098, doi:10.1029/2000JD900324.
- Glaccum, R. A., and J. M. Prospero (1980), Saharan aerosols over the tropical North Atlantic—Mineralogy, *Mar. Geol.*, **37**, 295–321, doi:10.1016/0025-3227(80)90107-3.
- Gomes, L., G. Bergametti, G. Coudé-Gaussen, and P. Rognon (1990), Submicron desert dusts: A sandblasting process, *J. Geophys. Res.*, **95**, 13,927–13,935, doi:10.1029/JD095iD09p13927.
- Holben, B. N., et al. (1998), AERONET: A federated instrument network and data archive for aerosol characterization, *Remote Sens. Environ.*, **66**(1–16), doi:10.1016/S0034-4257(98)00031-5.
- Maring, H., D. L. Savoie, M. A. Izaguirre, L. Custals, and J. S. Reid (2003), Mineral dust aerosol size distribution change during atmospheric transport, *J. Geophys. Res.*, **108**(D19), 8592, doi:10.1029/2002JD002536.
- Marshall, I. A., J. P. Mitchell, and W. D. Griffiths (1991), The behavior of regular-shaped non-spherical particles in a TSI aerodynamic particle sizer, *J. Aerosol Sci.*, **22**, 73–89, doi:10.1016/0021-8502(91)90094-X.
- Miller, S. D., A. P. Kuciauskas, M. Liu, Q. Ji, J. S. Reid, D. W. Breed, A. L. Walker, and A. A. Mandoos (2008), Haboob dust storms of the southern Arabian Peninsula, *J. Geophys. Res.*, **113**, D01202, doi:10.1029/2007JD008550.
- Noll, K. E., K. Y. P. Fang, and L. A. Watkins (1988), Characterization of the deposition of particles from the atmosphere to a flat plate (1988), *Atmos. Environ.*, **22**, 1461–1468, doi:10.1016/0004-6981(88)90170-9.
- Patterson, E. M. (1977), Commonalities in measured size distributions for aerosols having a soil derived component, *J. Geophys. Res.*, **82**, 2074–2082, doi:10.1029/JC082i015p02074.
- Perry, K. D., T. A. Cahill, R. C. Schnell, and J. M. Harris (1999), Long-range transport of anthropogenic aerosols to the National Oceanic and Atmospheric Administration baseline station at Mauna Loa Observatory, Hawaii, *J. Geophys. Res.*, **104**(D15), 18,521–18,534, doi:10.1029/1998JD100083.
- Peters, T. M. (2006), Use of the aerodynamic particle sizer to measure ambient PM10–2.5: The coarse fraction of PM10, *J. Air Waste Manage. Assoc.*, **56**, 411–416.
- Pierangelo, C., M. Mishchenko, Y. Balkanski, and A. Chédin (2005), Retrieving the effective radius of Saharan dust coarse mode from AIRS, *Geophys. Res. Lett.*, **32**, L20813, doi:10.1029/2005GL023425.
- Prospero, J. M. (1981), Eolian transport to the world ocean, in *The Sea*, vol. 7, *The Oceanic Lithosphere*, edited by C. Emiliani, pp. 801–874, John Wiley, New York.
- Prospero, J. M., M. Uematsu, and D. L. Savoie (1989), Mineral aerosol transport to the Pacific Ocean, in *Chemical Oceanography*, vol. 10, edited by J. P. Riley, pp. 187–218, Academic, San Diego, Calif.
- Quinn, P. K., et al. (2004), Aerosol optical properties measured on board the Ronald H. Brown during ACE-Asia as a function of aerosol chemical composition and source region, *J. Geophys. Res.*, **109**, D19S01, doi:10.1029/2003JD004010.
- Reid, J. S. (1993), Advanced physical methods for aerosol characterization with applications to Kuwait and Owens (dry) Lake, M. S. thesis, Univ. of Calif., Davis, Dec.
- Reid, J. S., and T. M. Peters (2007), Update to “Reconciliation of coarse mode sea-salt aerosol particle size measurements and parameterizations at a subtropical ocean receptor site” regarding the use of aerodynamic particle sizers in marine environments, *J. Geophys. Res.*, **112**, D04202, doi:10.1029/2006JD007501.
- Reid, J. S., R. G. Floccchini, T. A. Cahill, R. S. Ruth, and D. P. Salgado (1994), Local meteorological, transport, and source aerosol characteristics of late Autumn Owens Lake (dry) dust storms, *Atmos. Environ.*, **28**, 1699–1706, doi:10.1016/1352-2310(94)90315-8.
- Reid, J. S., H. H. Jonsson, H. B. Maring, A. A. Smirnov, D. L. Savoie, S. S. Cliff, E. A. Reid, M. M. Meier, O. Dubovik, and S.-C. Tsay (2003), Comparison of size and morphological measurements of coarse mode dust particles from Africa, *J. Geophys. Res.*, **108**(D19), 8593, doi:10.1029/2002JD002485.
- Reid, J. S., B. Brooks, K. K. Crahan, D. A. Hegg, T. F. Eck, N. O'Neill, G. de Leeuw, E. A. Reid, and K. D. Anderson (2006), Reconciliation of coarse mode sea-salt aerosol particle size measurements and parameterizations at a subtropical ocean receptor site, *J. Geophys. Res.*, **111**, D02202, doi:10.1029/2005JD006200.
- Reid, J. S., et al. (2008), An overview of UAE² flight operations: Observations of summertime atmospheric thermodynamic and aerosol profiles of the southern Arabian Gulf, *J. Geophys. Res.*, doi:10.1029/2007JD009435, in press.
- Slinn, S. A., and W. G. N. Slinn (1980), Predictions for particle deposition on natural waters, *Atmos. Environ.*, **14**, 1013–1016.
- Stein, S. W., B. J. Gabrio, D. Oberreit, P. Hairston, P. B. Myrdal, and T. J. Beck (2002), An evaluation of mass-weighted size distribution measurements with the Model 3320 aerodynamic particle sizer, *Aerosol Sci. Technol.*, **36**, 845–854, doi:10.1080/02786820290092087.
- Volckens, J., and T. M. Peters (2005), Counting and particle transmission efficiency of the aerodynamic particle sizer, *J. Aerosol Sci.*, **36**, 1400–1408, doi:10.1016/j.jaerosci.2005.03.009.
- Wang, J., et al. (2002), Clear-column radiative closure during ACE-Asia: Comparison of multiwavelength extinction derived from particle size and composition with results from Sun photometry, *J. Geophys. Res.*, **107**(D23), 4688, doi:10.1029/2002JD002465.
- Zhu, M., and M. Atkinson (2004), Observed and modeled climatology of the land-sea breeze circulation over the Persian Gulf, *Int. J. Climatol.*, **24**, 883–905, doi:10.1002/joc.1045.

A. Al Mandoos, Department of Atmospheric Studies, Ministry of Presidential Affairs, P.O. Box 4815, Abu Dhabi, United Arab Emirates.

S. Cliff, Department of Land, Air and Water Resources, University of California, Davis, CA 95616, USA.

T. F. Eck and S.-C. Tsay, NASA Goddard Space Flight Center, Greenbelt, MD 20771, USA.

S. Piketh, Climatology Research Group, University of Witwatersrand, Private Bag 2050, WITS 2050, Johannesburg, South Africa.

E. A. Reid, J. S. Reid, and A. Walker, Marine Meteorology Division, Naval Research Laboratory, 7 Grace Hopper Avenue, Stop 2, Monterey, CA 93943-5502, USA. (jeffrey.reid@nrlmry.navy.mil)